M. Trieschmann
G. Spital
A. Lommatzsch
E. van Kuijk
F. Fitzke
A. C. Bird
D. Pauleikhoff

# Macular pigment: quantitative analysis on autofluorescence images

M. Trieschmann · G. Spital
A. Lommatzsch · D. Pauleikhoff (✉)
Department of Ophthalmology,
St. Franziskus Hospital,
Hohenzollernring 74, 48145 Münster,
Germany
e-mail: dapauleikhoff@muenster.de

E. van Kuijk
University of Texas Medical Branch,
Galveston, USA

F. Fitzke
Department of Visual Science,
Institute of Ophthalmology, London, UK

A. C. Bird
Moorfields Eye Hospital, London, UK

**Abstract** *Background:* Macular pigment (MP) reduces oxidative damage in the central retina and can be quantified by flicker-photometric analysis (HFP) of MP optical density. These analyses demonstrate a very good correlation with central absorption by MP on autofluorescence (AF) images. With these techniques different types of MP-distribution have been described. In the present study a quantification analysis of MP in AF images was developed to verify these MP types and to compare MP distribution patterns between healthy individuals and those with age-related macular degeneration (AMD). *Methods:* AF images (HRA) were analysed with respect to the area of central and paracentral absorption in 400 eyes with a computerised analysis program of MP optical density. The patients were between 41 and 90 years old (mean 67.2 years); 168 were male and 232 female, and 253 had early AMD and 147 showed no AMD characteristics. The central MP concentrations (peak) were measured, the amount of MP values within the first 8-pixel radius ("C"), the total amount of MP within a 120-pixel radius ("T") were calculated as the volume of the MP values over the regarded radius and the C/T ratio was registered. *Results:* Four types of MP distribution (type 1, intense central and paracentral MP; type 2, less intense central and paracentral MP; type 3, only central MP; type 4, only paracentral MP) were identified. The differences in MP distribution were confirmed and clearly characterised by quantitative analyses of peak, total MP ("T"), central MP ("C") and C/T ratio: mean peak in type 1, 0.65; type 2, 0.42; type 3, 0.42; type 4, 0.29; mean total amount of MP in 120-pixel radius ("T") in type 1, 5829.0; type 2, 4412.5; type 3, 2709; type 4, 4302.8. MP types with lower levels of MP were significantly more often observed in the AMD group (AMD: type 1, 120=47.4%; types 2–4, 133=52.6%; healthy eyes: type 1, 112=76.2%; types 2–4, 35=23.8%) ($P<0.0001$) *Conclusions:* Analysis of MP on AF images is a quantitative method for investigation of MP. With this method a wide variation in concentration and distribution of MP could be seen in the population. Four different types of MP distribution could be characterised and quantitatively distinguished. Reduced levels of MP seem to be associated with a higher risk of development of AMD as they were significantly more often observed in the AMD group. This strategy of quantitative MP analysis on AF images is easily practicable and may be used in further studies to investigate the role of MP as a potential risk factor for AMD.

## Introduction

The growing evidence that high levels of carotenoids in the diet and in blood plasma are associated with a lower risk for age related macular degeneration[15, 33] has lead to various attempts to measure the levels of macular pigment in vivo in order to create an individual risk profile [3, 9, 14, 25, 32, 42].

The macular pigment (MP) consists of lutein and zeaxanthin [8, 10, 37].These carotenoids cannot be synthesised by mammals, and are therefore of dietetic origin. They reduce the effects of chromatic aberration and have light-absorbing properties with absorption spectra in the 400–540 nm range, the maximum absorption occurring at approximately 460 nm, whereby they are believed to protect photoreceptor cells from light damage by absorbing shorter wavelengths [34]. Furthermore, the MP has a direct antioxidative effect by neutralising cytotoxic free radicals generated by the light absorption process [2, 20, 28].

The highest levels of lutein and zeaxanthin are measured in the centre of the fovea. The concentrations decrease with eccentricity—at about 2 mm distance from the centre little MP is detected. Histologically, the MP is mainly localised in the axons of the cone receptors and only 25% is in the rod and cone outer segments [31, 35]. Histological analyses showed that zeaxanthin levels decrease more steeply than those of lutein with increasing eccentricity. Zeaxanthin molecules prevail in the cones, lutein molecules in the rod outer segments, and thereby lutein is predominant in the perifoveal zone [9, 31, 36, 37].

On histological analyses a high degree of variation in the foveal and parafoveal distribution of MP between individuals with a range of MP between 200–900 μm was revealed. The predominant localisation of MP was in the inner foveal retina in the photoreceptor axons [29].

Flicker-photometric analysis and the absorption in autofluorescence (AF) images are thought to indicate the amount of MP. The lipofuscin granules at the level of the retinal pigment epithelium absorb blue light and emit it as green AF. In areas with MP the blue light is absorbed by the carotenoids. These areas show reduced light intensity on AF imaging. Because Robson et al. demonstrated a good correlation of results between psychophysical, flicker-photometric MP analysis and AF images with regard to peak density and spatial distribution [32], the values measured on AF analysis can be used to define the individual MP concentration.

## Material and methods

Images of fundus AF were obtained in 400 persons between 41 and 90 years of age (mean 67.2 years) with and without macular disease using a confocal scanning laser ophthalmoscope, the Hei-delberg retina angiograph (HRA). Among these were 168 male and 232 female probands; 253 showed signs of early age-related macula degeneration (AMD; drusen, RPE proliferation, atrophy) and 147 showed no signs of AMD. Eyes with central atrophic spots as well as those with central RPE proliferation were excluded from the study because these features affect the measurement of AF. In all subjects one eye was selected and levels of fundus AF were recorded. None of the subjects involved in the study had ever taken lutein or zeaxanthin supplementation.

Images of fundus AF were obtained after pupil dilatation, taking 12 images of each eye and aligning them to scale down artefacts resulting from eye movement. Anatomical landmarks such as retinal blood vessels were used as reference points for accurate alignment and averaging [40, 41, 42].

The HRA uses confocal laser scanning and detection technology to acquire digital images. An argon ion laser (488 nm wavelength) is used for investigation of AF. Barrier filters at 500 nm and 810 nm provide fluorescence light detection.

The intensity and spatial distribution of fundus AF is documented and it is presumed that the attenuation of the AF in the centre is proportional to the amount of blue light-absorbing MP.

In the centre of the fovea the AF usually is most strongly attenuated. In perifoveal sites the AF increases gradually, until finally the normal AF due to lipofuscin is measured.

Relative optical density values are derived from the mean grey scale intensity annularly around the fovea.

In order to analyse the topographic distribution of the MP with the help of fundus AF method the following computer program was designed:

First the upper and lower limits are defined. Then we stretch the intensities of the image's pixels between these limits. The lower limit is determined by the average grey value of the 0.1% darkest pixels of the whole image. These pixels are localised inside the papilla or over a blood vessel. The upper limit is determined by the average grey value of the 5% brightest pixels of the whole image. If the image is evenly illuminated then these pixels are localised in circular fashion around the macula.

We then determine the average grey value of all pixels of the image that have the same distance to the fovea. We calculate the optical density by means of the following formula:

$$OD = Log\left(\frac{I_{Max} - I_{Min}}{I - I_{Min}}\right)$$

$I_{Max}$ is the upper limit in the normalised image; $I_{Min}$ is the lower limit in the normalised image; $I$ is the averaged grey value for all pixels with a given distance to the fovea.

The values for OD are computed for all distances to the fovea (radii) from 0 to 160 pixels (roughly 9.3° radius). These values are afterwards displayed in a diagram. We averaged the pixels with all their neighbours within 1° radius before calculating the optical density.

Figure 1 shows an AF image and its optical density diagram that was obtained using this method. The distance (x-axis) is measured in pixels. Seventeen pixels are about 1°. The red line displays the averaged optical density at every distance. The green bars display its standard deviation, and the blue bars display its maximum and minimum optical density.

Four hundred eyes of 400 individuals were examined with AF imaging and the optical density values were computed.

To obtain a better comparability of the MP values uniformly in each picture the first measuring point is set at the centre of the fovea, the second mark is set at 8-pixel radius (i.e. 150 μm) and the plateau, the site where the MP is presumed to be absent, is set at 120 pixels (i.e. 2 mm in 30° pictures). Afterwards the maximum central MP value—this value was in former studies called the peak—and the MP value at 8-pixel radius are determined. Furthermore, the total amount of MP in 120 pixel (2 mm, 7°) radius (total MP volume) and also the amount of MP in the central 8-pixel

**Fig. 1** HRA autofluorescence image and optical density. The diagram on the *right* shows the optical density versus the distance to the fovea in pixels: the *red line* shows the averaged optical density; the *green bar* shows the standard deviation of the optical density; the *blue bar* shows the minimum and maximum optical density for a given radius
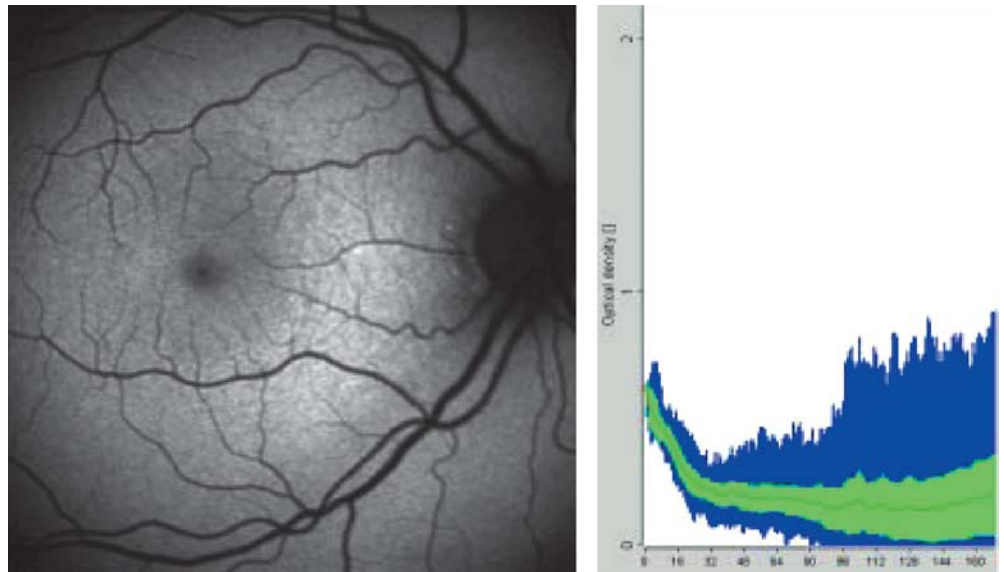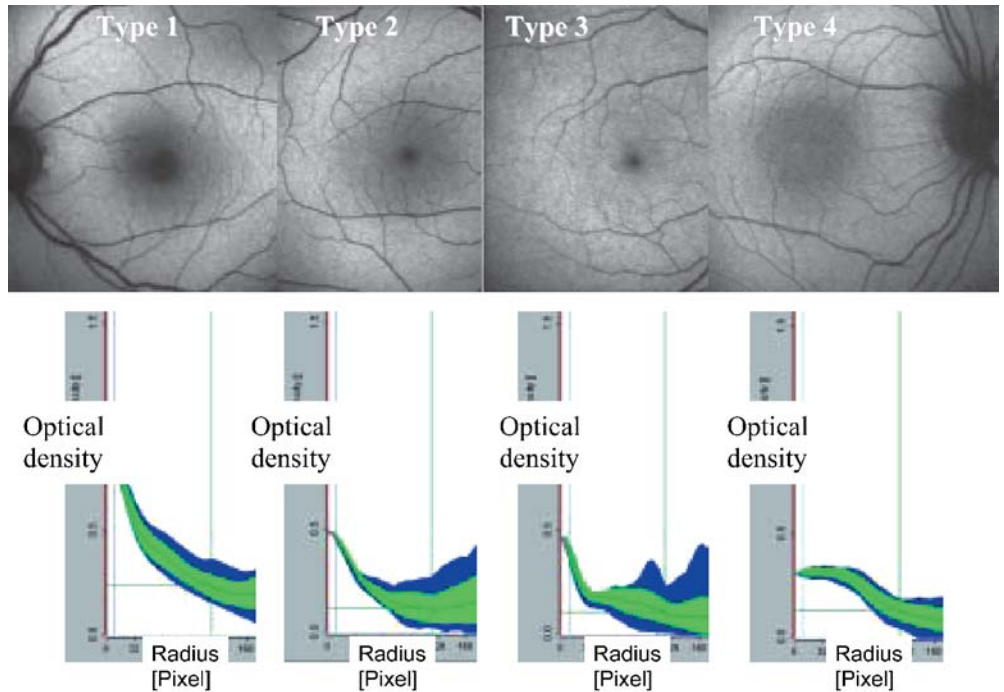


**Fig. 2** The four types of autofluorescence distribution



(150-µm) radius (central MP volume) are computed as the volume of the optical density values in the regarded radius. The C/T ratio is calculated as (central MP volume):(total MP volume).

## Results

The presented technique for measuring MP based on AF pictures of 400 probands showed variation of the distribution and amount of MP in the foveal and perifoveal sites. As van Kuijk et al. showed, the various spatial profiles of

AF throughout the posterior pole can be divided into phenotypes 1–4 [38]. The presented method of analysis of MP concentrations offers a quantitative verification of the subjective classification of the different MP types.

### Type 1

Type 1 shows a dark central hypofluorescence of greater than 150 µm radius surrounded by a lighter peripheral hypofluorescence (Fig. 2).

**Table 1** Type 1 shows the highest central concentration of MP (peak), type 4 the lowest (*P*<0.0001)

| Central MP peak | Type 1 n=232 | Type 2 n=126 | Type 3 n=17 | Type 4 n=25 |
|---|---|---|---|---|
| Maximum | 1.1 | 0.62 | 0.72 | 0.42 |
| Minimum | 0.36 | 0.15 | 0.28 | 0.1 |
| Mean | 0.65 | 0.42 | 0.42 | 0.29 |

**Table 2** Type 1 shows the highest amounts of MP within the first 8 pixels (C; 150 μm radius) (central MP volume) (*P*<0.0001)

| Central MP volume | Type 1 n=232 | Type 2 n=126 | Type 3 n=17 | Type 4 n=25 |
|---|---|---|---|---|
| Maximum | 312.6 | 170.2 | 157.2 | 122.4 |
| Minimum | 89.7 | 41.2 | 59.6 | 28.7 |
| Mean | 168.4 | 107.8 | 112 | 79 |

**Table 3** Type 1 has the highest amount of total MP volume in 120 pixels (T), type 3 the lowest (*P*<0.0001)

| Total MP volume | Type 1 n=232 | Type 2 n=126 | Type 3 n=17 | Type 4 n=25 |
|---|---|---|---|---|
| Maximum | 13182.3 | 9713 | 4061.3 | 6761.2 |
| Minimum | 2513.1 | 1539.9 | 157.3 | 1485.8 |
| Mean | 5829.0 | 4412.5 | 2709 | 4302.8 |

**Table 4** The C/T ratio is highest in type 3, lowest in type 4

| C/T ratio | Type 1 n=232 | Type 2 n=126 | Type 3 n=17 | Type 4 n=25 |
|---|---|---|---|---|
| Maximum | 1.6% | 1.0% | 3.2% | 1.2% |
| Minimum | 5.4% | 4.3% | 4.9% | 2.8% |
| Mean | 2.9% | 2.5% | 4.2% | 1.9% |

The optical density curve shows high central levels of MP, high central MP volume (volume of optical density values over 8-pixel radius) corresponding to the big dark spot seen in the AF image. These values and also the total MP volume are the highest of the four types (Tables 1, 2, 3, 4). Type 1 is most common in healthy subjects.

### Type 2

Type 2 features lowered central MP and total MP and shows a central lowered AF of less than 150 μm radius surrounded by a lighter peripheral hypofluorescence (Fig. 2).

Compared to type 1, the optical density curve shows lower levels of central MP, a shallow curve progression, lower amounts of central MP volume and also lower amounts of total MP volume (Tables 1, 2, 3, 4).

**Table 5** Prevalence of the four MP phenotypes in healthy and AMD individuals (*P*<0.0001)

| | Type 1 | Type 2 | Type 3 | Type 4 |
|---|---|---|---|---|
| Healthy eyes (n=147) | 76.2% n=122 | 19.7% n=29 | 2.04% n=3 | 2.04% n=3 |
| AMD (n=253) | 47.4% n=120 | 38.3% n=97 | 5.5% n=14 | 8.7% n=22 |

### Type 3

Type 3 has only central MP, no pericentral MP and typically has only a central hypofluorescence of less than 150 μm radius with no peripheral hypofluorescence distinguishable from the background (Fig. 2). The optical density curve shows a bend at the point where the central dark spot of the AF image ends and the peripheral AF begins. The total amount of MP is the lowest of the four types.

The C/T ratio is the highest of the four types, representing the fact that only central MP can be detected and almost no surrounding MP can be presumed (Tables 1, 2, 3, 4) .

### Type 4

Type 4 shows no enhanced central hypofluorescence compared with pericentral hypofluorescence, but increased hypofluorescence in the macula relative to the background (Fig. 2).

The optical density curve shows the lowest central MP values and the lowest central MP volume. The C/T quotient also is the lowest of all four types, corresponding to the fact that only peripheral MP is observed and no central accumulation of MP is detected.

The subdivision into four types of MP based on distribution of fundus AF was found to be fully represented in the quantitative analyses of the grey scale values (Tables 1, 2, 3, 4).

### Prevalence of MP types in healthy and AMD individuals

In healthy eyes without signs of AMD, type 1 prevails (76.2%) (*P*<0.0001). Subjects with AMD showed significantly more often types 2–4 with lower levels of MP than the healthy subjects did (AMD: type 1, 120=47.4%; types 2–4, 133=52.6%, healthy eyes: type 1, 112=76.2%; types 2–4, 35=23.8%) (Table 5).

In 80 individuals the MP distribution in the fellow eye was investigated. A symmetry of the MP distribution was found in 86%.

## Discussion

Growing interest in the relationship between MP and the development or progression of AMD has lead to various attempts to assess MP[3, 9, 14, 25, 32, 42].

In recent studies the MP was measured employing psychophysical methods based on heterochromatic flicker photometry. These measurements assess the central maximum concentration compared with that in a reference location that lies beyond the lateral extent of MP [1, 2, 3, 4, 16, 17, 18, 22, 23, 30], but none of them reflect the spatial distribution of MP and its interindividual variability [19, 26, 27, 39] .The central concentration of MP does not always correlate with the total amount of MP an individual has [19, 26, 27, 32].

Currently the influence of irregular lipofuscin distribution in the RPE on analyses of the AF pattern cannot fully be assessed. Local hypofluorescence may be due to a high level of blue light-absorbing MP and/or it may be a consequence of decreased emission by locally reduced levels of lipofuscin. The amount and allocation of MP can be overestimated in AF imaging on the basis of absorption characteristics of melanin in the RPE or of haemoglobin or the crystalline lens. Effects of these variables have been investigated employing longer wavelengths that are not absorbed by MP (550 nm)[14]. The optical density of MP showed a positive correlation with the melanin density difference determined by reflectometry. The average overestimation in the MP densities was quantified arithmetically as 0.07±0.05 density units. This may influence the lower levels of MP on AF images, but because the standard deviation was relatively large in each group, the influence of an overestimation in eyes with lower MP should be limited.

In general, the close correlation between MP concentrations measured with the help of psychophysical methods and with AF imaging [25, 32] suggests that the dark areas of AF are primarily the consequence of absorption features of MP.

AF imaging can therefore be used to estimate the distribution of Mp in the human retina in vivo. The AF imaging offers a kind of map of MP distribution at the posterior pole. The darker foveal area in AF images of the posterior pole corresponds to the amount of MP present.

The investigation of the fundus AF and the quantitative analysis of the intensity of blue light absorption by MP gives us a reproducible and objective method for the assessment of MP. The current study shows a high degree of interindividual variability in terms of peak MP and distribution in healthy individuals as well as in those with AMD.

These findings support the basis for the grading system developed for phenotyping of MP into four types [38] and the morphological features of these four phenotypes were characterised in the quantitative analysis of grey-scale values. The four types show differences in central and paracentral MP distribution with decreasing concentration of MP from type 1 to the other types.

All images were analysed according to their morphological features, employing a modified grid as already known from analyses of different AMD stages [7, 13, 21]. This grid, reduced to a central ring of 150 μm radius, can be used to differentiate between the four phenotypes of MP distribution. Therefore, although the four phenotypes probably represent a continuous spectrum, the differentiation of the central amount and lateral extent of MP may describe specific properties of this spectrum and produce clusters of possible MP distribution.

Both eyes of one individual were examined in 80 persons and the MP distribution showed symmetry in 86% of cases. The intraindividual symmetry of the MP allocation is likely to reflect environmental or genetic attributes that regulate the amount and distribution of MP.

Prognostic implication of this study

Subjects with AMD showed significantly more often phenotypes 2–4 with lower levels of MP than healthy subjects did. A lower amount of MP seems to be associated with an increased risk of AMD development [1, 4, 11, 22, 23].These relationships have to be qualified in further studies.

Especially types 3 and 4 were found to be very rare in healthy subjects, whereas they were more often observed in the AMD group, which may indicate that types 3 and 4 represent a state of increased risk for AMD development. As biochemical studies showed that zeaxanthin is predominant in the foveal zone, type 4 may have a lag of zeaxanthin, while type 3 could have an amount of lutein that lies below the detectable level using the presented method. Whether supplementation of one of the carotenoids [5, 6, 12, 19, 24] may change morphological features of MP distribution will be investigated in the future.

Fundus AF analysis provides a fast, non-invasive method of assessing differences in MP density. The four phenotypes of MP distribution and their quantitative analysis may be used in further clinical studies to evaluate the specificity of the association between MP concentrations and status of AMD observed.

## Appendix: Analysis

Let $F_F (\Lambda,\lambda)$ and $F_P (\Lambda,\lambda)$ be the AF ($\Lambda$ is the excitation wavelength, $\lambda$ the emission wavelength) measured at the fovea and the perifovea, let $D_F$ and $D_P$ be the optical density of MP at both sites, and $F^*_F (\Lambda,\lambda)$ and $F^*_P (\Lambda,\lambda)$ be the fluorescence of all layers located posteriorly to the MP. We assume that all detected fluorescence has been affected by MP absorption and modify Delori's formula as follows (as due to the broad band-pass barrier filter we measure all wavelengths from 500 to 720 nm that reach the detec-

tor, not just a single wavelength as used in recent studies [14] Furthermore, we consider the spectral responsivity $S(\lambda)$ of the detector. Thus we can express the foveal and perifoveal fluorescence as:

$$F_F(\Lambda) = \int_{500}^{720} S(\lambda) * F_F^*(\Lambda,\lambda) * 10^{-D_F(\Lambda)-D_F(\lambda)} d\lambda =$$
$$10^{-D_F(\Lambda)} * \int_{500}^{720} S(\lambda) * F_F^*(\Lambda,\lambda) * 10^{-D_F(\lambda)} d\lambda \quad (1)$$

$$F_P(\Lambda) = \int_{500}^{720} S(\lambda) * F_P^*(\Lambda,\lambda) * 10^{-D_P(\Lambda)-D_P(\lambda)} d\lambda =$$
$$10^{-D_P(\Lambda)} * \int_{500}^{720} S(\lambda) * F_P^*(\Lambda,\lambda) * 10^{-D_P(\lambda)} d\lambda \quad (2)$$

Now we determine the logarithm of the quotient of Eq. 2 and Eq.1:

$$Log\left(\frac{F_P(\Lambda)}{F_F(\Lambda)}\right) =$$
$$D_F(\Lambda) - D_P(\Lambda) + Log\left(\frac{\int_{500}^{720} S(\lambda) * F_P^*(\Lambda,\lambda) * 10^{-D_P(\lambda)} d\lambda}{\int_{500}^{720} S(\lambda) * F_F^*(\Lambda,\lambda) * 10^{-D_F(\lambda)} d\lambda}\right) \quad (3)$$

Applying Beer's law we get:

$$Log\left(\frac{F_P(\Lambda)}{F_F(\Lambda)}\right) = D_{AF}(460) * K_{MP}(\Lambda)$$
$$+ Log\left(\frac{\int_{500}^{720} S(\lambda) * F_P^*(\Lambda,\lambda) * 10^{-D_P(\lambda)} d\lambda}{\int_{500}^{720} S(\lambda) * F_F^*(\Lambda,\lambda) * 10^{-D_F(\lambda)} d\lambda}\right) \quad (4)$$

If we neglect the log term ($F_P^*(\Lambda,\lambda) \approx F_F^*(\Lambda,\lambda)$) and $D_P(\lambda)\approx 0$ and $D_F(\lambda)\approx 0$ for most of the detected wavelengths) on the right side we get:

$$Log\left(\frac{F_P(\Lambda)}{F_F(\Lambda)}\right) = D_{AF}(460) * K_{MP}(\Lambda) \quad (5)$$

or

$$D_{AF}(460) = Log\left(\frac{F_P(\Lambda)}{F_F(\Lambda)}\right) * \frac{1}{K_{MP}(\Lambda)} \quad (6)$$

If we consider the extinction coefficient for $\Lambda$=488 nm we get:

$$D_{AF}(460) = Log\left(\frac{F_P(\Lambda)}{F_F(\Lambda)}\right) * 1.3 \quad (7)$$

Let C be the brightest spot on the image. Applying the rules of logarithm we can calculate:

$$D_{AF}(460) = Log\left(\frac{F_P(\Lambda)}{F_F(\Lambda)}\right) * 1.3 + 0 * 1.3 =$$
$$Log\left(\frac{F_P(\Lambda)}{F_F(\Lambda)}\right) * 1.3 + Log\left(\frac{F_C(\Lambda)}{F_C(\Lambda)}\right) * 1.3 =$$
$$Log\left(\frac{F_C(\Lambda)}{F_F(\Lambda)}\right) * 1.3 - Log\left(\frac{F_C(\Lambda)}{F_P(\Lambda)}\right) * 1.3 \quad (8)$$

This means we can calculate the optical density relatively to the brightest spot in each image. Then we have to subtract the optical density of the plateau from this value to get the optical density of the fovea relative to the plateau. First we determine the radial distribution of the optical density around the fovea. Since we want the location of the plateau to be variable, we normalise the optical densities to the brightest spot in the image and display it.

Now the plateau is marked. Using Eq. 8 we subtract the optical density of the plateau to get the values relative to the plateau. These values are evaluated, averaged, integrated and so on.

# References

1. Beatty S, Boulton M, Henson D, Koh HH, Murray IJ (1999) Macular pigment and age related macular degeneration. Br J Ophthalmol 83:867–877
2. Beatty S, Koh H, Phil M, Henson D, Boulton M (2000) The role of oxidative stress in the pathogenesis of age-related macular degeneration. Surv Ophthalmol 45:115–134
3. Beatty S, Koh HH, Carden D, Murray IJ ( 2000) Macular pigment optical density measurement:a novel compact instrument . Ophthalmic Physiol Opt 20:105–111
4. Beatty S, Murray IJ, Henson DB, Carden D, Koh HH, Boulton ME (2001) Macular pigment and risk for age-related macular degeneration in subjects from a northern European population. Invest Ophthalmol Vis Sci 42:439–446
5. Berendschot TT, Willemse-Assink JJ,Bastiaanse M, de Jong PT, van Norren D (2002) Macular pigment and melanin in age-related maculopathy in a general population. Invest Ophthalmol Vis Sci 43:1928–1932
6. Berendschott TJ, van de Kraats J, van Norren D (2001) Wavelength dependence of the Stiles–Crawford effect explained by perception of backscattered light from the choroids.J Opt Soc Am A Opt Image Sci Vis 18:1445–51
7. Bird AC, Bressler NM, Bressler SB, Chisholm IH, Coscas G, Davis MD, de Jong PT, Klaver CC, Klein BE, Klein R, et al (1995) An international classification and grading system for age related maculopathy in age-related macular degeneration. Surv Ophthalmol 39:367–374
8. Bone RA, Landrum JT, Tarsis SL (1985) Preliminary identification of the human macular pigment. Vision Res 25:1531–1535
9. Bone RA, Landrum JT, Fernandez L (1988) Analysis of the macular pigment by HPLC: retinal distribution and age study. Invest Ophthalmol Vis Sci 29:843–849
10. Bone RA, Landrum JT, Friedes LM (1997) Distribution of lutein and zeaxanthin stereoisomers in the human retina. Exp Eye Res 64:211–218
11. Bone RA, Landrum JT, Mayne ST, Gomez CM, Tibor SE, Twaroska EE (2001) Macular pigment in donor eyes with and without AMD. A case-control study. Invest Ophthalmol Vis Sci 42:235–240
12. Ciulla TA,Curran-Celentano J, Cooper DA et al (2001) Macular pigment optical density in a midwestern sample. Ophthalmology 108:350–355
13. Curcio CA, Medeiros NE, Millican CL (1998) The Alabama Age-related Macular Degeneration Grading system for donor eyes Invest Ophthalmol Vis Sci 39:1085–1096
14. Delori FC, Goger DG, Hammond BR, Snodderley DM, Burns SA (2001) Macular pigment density measured by AF spectrometry: comparison with reflectometry and heterochromatic flicker photometry. J Opt Soc Am A 18:1212–1230
15. Eye Disease Case-Control Study Group (1993) Arch Ophthalmol 111:104–109
16. Hammond BR, Caruso-Avery M (2000) Macular pigment optical density in a southwestern sample. Invest Ophthalmol Vis Sci 41:1492–1497
17. Hammond BR, Fuld K (1992) Interocular differences in macular pigment density. Invest Ophthalmol Vis Sci 33:350–355

18. Hammond BR, Fuld K, Snodderly DM (1996) Iris colour and macular pigment optical density. Exp Eye Res 62:715–720

19. Hammond BR, Johnson EJ, Russell RM et al (1997) Dietary modification of human macular density. Invest Ophthalmol Vis Sci 38:1795–1801

20. Kirschfield K (1982) Carotenoid pigments: their possible role in protecting against photooxidation in eyes and photoreceptor cells. Proc R Soc Lond B 216:71–85

21. Klein R, Davis MD, Magli YL, Segal P,Klein BEK, Hubbard L (1991) The Wisconsin age-related maculopathy grading system. Ophthalmology 98:1128–1134

22. Landrum JT, Bone RA, Vidal I, Menendez E, Kilburn M (1995) Macular pigment stereomers in individual eyes: a comparison between normals and those with age-related macular degeneration. Invest Ophthalmol Vis Sci 36 [Suppl]: 857–863

23. Landrum JT,Bone RA,Kilburn MD (1997) The macular pigment—a possible role in protection from age related macular degeneration. Adv Pharmacol 38:537–556

24. Leung I, Tso M, Li W, Lam T (2001) Absorption and tissue distribution of zeaxanthin and lutein in rhesus monkeys after taking Fructus lycii (Gou Qi Zi) extract. Invest Ophthalmol Vis Sci 42:466–471

25. Lois N, Halfyard AS, Bird AC, Fitzke FW (2000) Quantitative evaluation of fundus autofluorescence imaged "in vivo" in eyes with retinal disease. Br J Ophthalmol 84:741–745

26. Moreland JD, Bhatt P (1984) Retinal distribution of retinal pigment. Doc Ophthalmol Proc Ser 39:127–132

27. Moreland JD, Robson AG, Soto-Leon N, Kulikowski JJ (1998) Macular pigment and the colour-specificity of visual evoked potentials. Vision Res 38:3241–3245

28. Nussbaum JJ, Pruett RC, Delori FC (1981) Macular yellow pigment. The first 200 years. Retina 1:296–310

29. Pauleikhoff D, van Kuijk FJGM, Alexander R, Luthert P, Bird AC (2002) Histological evaluation of localization and distribution of macular pigment in the human retina. Invest Ophthalmol Vis Sci [Suppl] S102

30. Pease PL, Adams AJ, Nuccio E (1987) Optical density of human macular pigment. Vision Res 27:705–710

31. Rapp LM, Maple SS, Choi JH (2000 ) Lutein and zeaxanthin concentrations in rod outer segment membranes from perifoveal and peripheral human retina.Invest Ophthalmol Vis Sci 41:1200–1209

32. Robson AG, Moreland JD, Pauleikhoff D, Morrissey T, Holder GE, Fitzke FW, C Bird A, van Kuijk FJ (2002) Macular pigment density and distribution: comparison of the fundus autofluorescence with minimum motion photometry. Vision Res 43:1765–75

33. Seddon JM, Ajani UA, Sperduto RD, Hiller R, Blair N, Burton TC, Farber MD, Gragoudas ES, Haller J, Miller DT, Yannuzzi LA, Willett W (1994) Dietary carotenoids, vitamins A, C, and E, and advanced age-related macular degeneration. Eye Disease Case-Control Study Group. J Am Med Assoc 272:1413–1420

34. Snodderly DM (1995) Evidence for protection against age-related macular degeneration by carotinoids and antioxidant vitamins. Am J Clin Nutr 62:1448–1461

35. Snodderly DM, Brown PK, Auran JD, Delori FC (1984) The macular pigment. I. Absorbance spectra, localisation and discrimination from other yellow pigments in primate retinas. Invest Ophthalmol Vis Sci 25:660–673

36. Snodderly DM, Handelmann GJ, Adler AJ (1991) Distribution of individual macular pigment carotenoids in central retina of macaque and squirrel monkeys. Invest Ophthalmol Vis Sci 32:268–279

37. Sommerburg O, Siems WG,Hurst JS, Lewis JW, Kliger DS, van Kuijk FGJM (1999) Lutein and Zeaxanthin are associated with photoreceptors in the human retina. Curr Eye Res 19:491–495

38. van Kuijk FJGM, Pelosini L, Patel J, Pauleikhoff D, Fitzke F, Bird AC: Grading of macular pigment phenotypes using autofluorescence imaging Invest Ophthalmol Vis Sci [Suppl] S102

39. Vienot F (1997) Effect of macular pigmentation and cone effective optical density on colour matches. XIVth Symposium IRGCVD, P25

40. Von Rückmann A, Fitzke FW, Bird AC (1995) Distribution of funds auto fluorescence with a scanning laser ophthalmoscope. Br J Ophthalmol 79:407–412

41. Von Rückmann A, Fitzke FW, Bird AC (1997) Fundus autofluorescence in age-related macular disease with a scanning laser ophthalmoscope. Invest Ophthalmol Vis Sci 38:478–486

42. Von Rückmann A, Fitzke FW, Bird AC (1999) Distribution of pigment epithelium auto fluorescence in retinal disease state recorded in vivo and its change over time. Graefes Arch Clin Exp Ophthalmol, 237:1-9